JAM CM Journal of Applied Mathematics and Computational Mechanics 2022, 21(3), 73-84
www.amcm.pcz.pl p-ISSN 2299-9965
DOI: 10.17512/jamcm.2022.3.06 e-ISSN 2353-0588

INVESTIGATION OF PROBABILISTIC ASPECTS RELIABILITY OF ISOTROPIC BODIES WITH INTERNAL DEFECTS

Roman Kvit

Department of Mathematics, Lviv Polytechnic National University
Lviv, Ukraine
kvit_rom@ukr.net

Received: 13 June 2022; Accepted: 9 September 2022

Abstract. A study of the stress state and reliability of an isotropic body with the same material crack resistance and evenly distributed internal defects-cracks under the conditions of homogeneous axisymmetric loading is carried out. Defects are characterized by two independent random variables – a radius and orientation angle. The probability density distribution of the defect radius is chosen in the form of an exponential law. The probability density distribution of the defect orientation angle is chosen in the form of a law that corresponds to the material isotropy. The influence of the loading level, type of stress state and body size (number of defects) on the most probable value, the mean value and the dispersion of failure loading (strength) are investigated.

MSC 2010: *74R10, 74R99, 60K35, 82C03*
Keywords: *fracture, reliability, distribution law, axisymmetric loading, disc-shaped crack, isotropic material*

1. Introduction

Research of reliability and construction of structural materials fracture criterion is an actual and important task. For high-strength materials, which in the operation process are characterized by brittle fracture, it is necessary to create reliable methods for predicting their properties. Taking into account the stochastic structure of brittle materials is an important component of effective modeling of their failure. The complex application of probabilistic-statistical methods and deterministic solutions of materials brittle fracture mechanics problems allows us to qualitatively model the strength and reliability of structural elements under different types of loading. In paper [1], a two-dimensional finite element simulation-based approach was developed to assess the pore-pore interactions and their impact on fracture statistics of isotropic microstructures. In article [2], the probabilistic fracture mechanical computing codes are compared. In work [3], strictly for statistical purposes, the microstructure of nacre is approximated by a diagonally pulled fishnet with quasibrittle

links representing the shear bonds between parallel lamellae (or platelets). The probability distribution of fishnet strength is calculated as a sum of a rapidly convergent series of the failure probabilities. A modified Weibull failure probability model that considers the impact of compressive stress on cladding failure probability is deduced, and then it is used to calculate the failure probability of different cladding designs [4]. In paper [5], a probabilistic procedure for modeling multiple surface crack propagation and coalescence is proposed. In the work [6], a data-driven approach based on a Gaussian process for regression is developed to determine the probability of axle failure caused by crack growth in railway axles. A reliability analysis of fatigue crack growth for a steel subject to the growth of multiple cracks is presented in [7].

The purpose of this study is to develop a comprehensive approach for calculating the reliability of stochastically defective bodies, which is based on the results of the fracture mechanics of materials with deterministic internal defects and data obtained by probabilistic methods.

2. Formulation of the problem

Consideration of internal defects in a three-dimensional body with their spatial location more adequately reflects the process of studying the solids (structural materials) strength. In this case, a disc-shaped (flat round in plan) crack, which is characterized by a radius and two angles of orientation in space is the simplest model. For the case of axisymmetric loading, we have two parameters – the radius R and the angle of orientation α between the normal $\vec{n}$ to the crack plane and the axis of symmetry Oz (Fig. 1). These parameters are statistically independent random variables and we can consider the laws of their probability distribution.

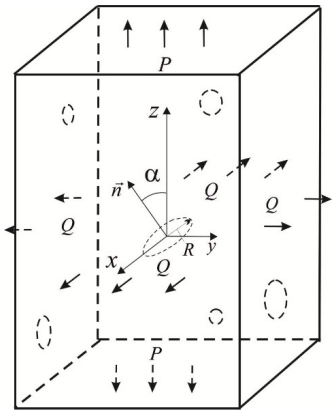

Fig. 1. Homogeneous axisymmetric loading of a stochastically defective body

Let us investigate a model of an elastic isotropic body (or its element) that has a volume V and the same material crack resistance K_{IC} under the conditions of

homogeneous axisymmetric loading P and $Q = \eta P$. Consider the uniform distribution of N disc-shaped defects-cracks (the number N is proportional to the volume V) that do not interact with each other.

According to the model material isotropy, the probability density distribution of random variable α is determined by the ratio $f(\alpha) = \sin\alpha$ $(0 \le \alpha \le \pi/2)$ [8].

In article [8], the probability density distribution of a random variable R was chosen in the form of a generalized β-distribution. In this study, we choose the probability density distribution of the R in the form of an exponential law [9]:

$$f(R) = \frac{1}{h} e^{-\frac{R}{h}}, \ (R \ge 0). \tag{1}$$

Here h is a distribution parameter that has a radius dimension. The corresponding probability distribution function is defined as follows:

$$F(R) = 1 - e^{-\frac{R}{h}}. \tag{2}$$

In Figure 2, the graph of a random variable R probability density distribution is constructed.

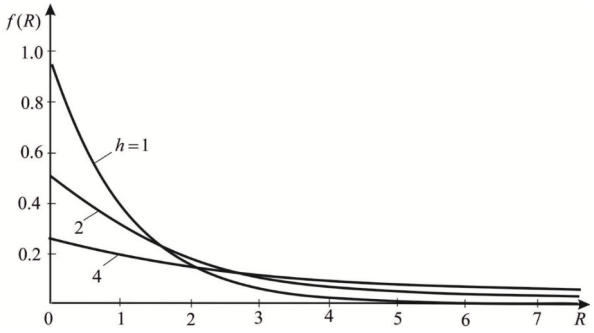

Fig. 2. The probability density distribution of a random variable R

The recorded distribution allows for the possibility of large radius cracks. As the value R increases, the probability of the defect presence decreases. This assumption simplifies the material model and mathematical calculations [10, 11].

3. Failure loading probability distribution function

In paper [12], the failure loading probability distribution function expressions for the case of choosing the random parameter R probability density distribution of a body element with one crack in the form of an exponential law (1), (2) are obtained. Write these expressions by entering an immeasurable loading $p = \frac{2P}{K_{IC}}\sqrt{\frac{h}{\pi}}$ for the following types of stress:

1) all-round tension for $P \geq Q \geq 0$ $(0 \leq \eta \leq 1)$

$$F_1(p,\eta) = \mathrm{T}_1(p,\eta) = e^{-p^{-2}} - \frac{1}{\sqrt{1-\eta}} \int_{p^{-2}}^{p^{-2}\eta^{-2}} e^{-x} \sqrt{\left(p\sqrt{x}\right)^{-1} - \eta}\, dx,\ 0 \leq p < \infty; \qquad (3)$$

2) all-round tension for $Q \geq P \geq 0$ $(1 \leq \eta < \infty)$

$$F_1(p,\eta) = \mathrm{T}_2(p,\eta) = e^{-p^{-2}} - \frac{1}{\sqrt{1-\eta}} \int_{p^{-2}\eta^{-2}}^{p^{-2}} e^{-x} \sqrt{\left(p\sqrt{x}\right)^{-1} - \eta}\, dx,\ 0 \leq p < \infty; \qquad (4)$$

3) tension in the axial and compression in the lateral directions for $P \geq 0$, $Q \leq 0$ $(-\infty < \eta \leq 0)$

$$F_1(p,\eta) = \mathrm{T}_3(p,\eta) = e^{-p^{-2}} - \frac{1}{\sqrt{1-\eta}} \int_{p^{-2}}^{\infty} e^{-x} \sqrt{\left(p\sqrt{x}\right)^{-1} - \eta}\, dx,\ 0 \leq p < \infty; \qquad (5)$$

4) compression in the axial and tension in the lateral directions for $P \leq 0$, $Q \geq 0$ $(-\infty < \eta \leq 0)$

$$F_1(-p,\eta) = \mathrm{T}_4(-p,\eta) = \frac{1}{\sqrt{1-\eta}} \int_{p^{-2}\eta^{-2}}^{\infty} e^{-x} \sqrt{\left(p\sqrt{x}\right)^{-1} - \eta}\, dx,\ 0 \leq -p < \infty. \qquad (6)$$

Based on the relations (3)-(6), it is possible to determine the body strength probabilistic characteristics.

The failure loading probability distribution function of a body element with one crack in partial cases is written like this:

1) the same all-round tension $(P = Q,\ \eta = 1)$

$$F_1(p,1) = e^{-p^{-2}},\ 0 \leq p < \infty; \qquad (7)$$

2) biaxial tension $\left(P = 0,\ q = \frac{2Q}{K_{Ic}}\sqrt{\frac{h}{\pi}} > 0,\ \eta \to \infty\right)$

$$F_1(q,\infty) = \int_{q^{-2}}^{\infty} e^{-x} \sqrt{1 - \left(q\sqrt{x}\right)^{-1}}\, dx,\ 0 \leq q < \infty; \qquad (8)$$

3) uniaxial tension $(P > 0,\ Q = 0,\ \eta = 0)$

$$F_1(p,0) = e^{-p^{-2}} - \int_{p^{-2}}^{\infty} e^{-x} \left(p\sqrt{x}\right)^{-1/2} dx,\ 0 \leq p < \infty; \qquad (9)$$

4) tension in axial and equal compression in the lateral directions ($P=-Q>0$, $\eta=-1$)

$$F_1(p,-1)=e^{-p^{-2}}-\frac{1}{\sqrt{2}}\int_{p^{-2}}^{\infty}e^{-x}\sqrt{1+\left(p\sqrt{x}\right)^{-1}}\,dx,\ 0\le p<\infty; \tag{10}$$

5) compression in the axial and equal tension in the lateral directions ($-P=Q>0$, $\eta=-1$)

$$F_1(-p,-1)=\frac{1}{\sqrt{2}}\int_{p^{-2}}^{\infty}e^{-x}\sqrt{1+\left(p\sqrt{x}\right)^{-1}}\,dx,\quad 0\le -p<\infty. \tag{11}$$

Figure 3 shows the curves of the failure loading probability distribution function $F_1(p,\eta)$ of a body element with one defect for some of the considered partial cases.

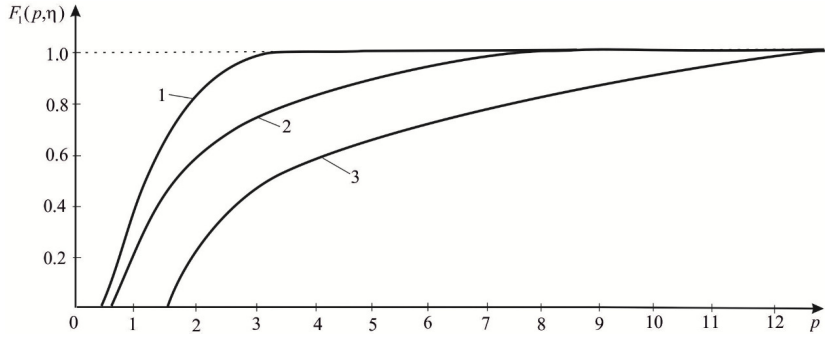

Fig. 3. Failure loading probability distribution function: 1 – the same all-round tension, 2 – biaxial tension, 3 – uniaxial tension

The failure loading probability distribution function $F_1(p,\eta)$ depends on the loading level p and the type of stress state (from η). The analysis shows that the function $F_1(p,\eta)$ increases with increasing magnitude p. As the parameter η changes, the shape of the graph of the function $F_1(p,\eta)$ changes.

4. Failure loading probability density distribution

The failure loading probability density distribution for a body with N defects is recorded as [13]:

$$f_N(p,\eta)=N(1-F_1(p,\eta))^{N-1}\frac{dF_1(p,\eta)}{dp}. \tag{12}$$

Substitute into formula (12) the expressions for the failure loading probability distribution function (3)-(6) and differentiate the integrals by parameter p. We get the expressions of failure loading probability density distribution $f_N(p,\eta)$:

1) all-round tension for $P \ge Q \ge 0$ $(0 \le \eta \le 1)$

$$f_N(p,\eta) = \frac{N\left(1-\mathrm{T}_1(p,\eta)\right)^{N-1}}{2p^2\sqrt{1-\eta}} \int\limits_{p^{-2}}^{p^{-2}\eta^{-2}} \frac{e^{-x}}{\sqrt{\left(p\sqrt{x}\right)^{-1}-\eta}} \frac{dx}{\sqrt{x}},\ 0 \le p < \infty; \tag{13}$$

2) all-round tension for $Q \ge P \ge 0$ $(1 \le \eta < \infty)$

$$f_N(p,\eta) = N\left(1-\mathrm{T}_2(p,\eta)\right)^{N-1} \left(\frac{4e^{-p^{-2}}}{p^3} + \frac{1}{2p^2\sqrt{1-\eta}} \int\limits_{p^{-2}\eta^{-2}}^{p^{-2}} \frac{e^{-x}}{\sqrt{\left(p\sqrt{x}\right)^{-1}-\eta}} \frac{dx}{\sqrt{x}} \right), \tag{14}$$

$0 \le -p < \infty$;

3) tension in the axial and compression in the lateral directions for $P \ge 0$, $Q \le 0$ $(-\infty < \eta \le 0)$

$$f_N(p,\eta) = \frac{N\left(1-\mathrm{T}_3(p,\eta)\right)^{N-1}}{2p^2\sqrt{1-\eta}} \lim_{b(p)\to\infty} \int\limits_{p^{-2}}^{b(p)} \frac{e^{-x}}{\sqrt{\left(p\sqrt{x}\right)^{-1}-\eta}} \frac{dx}{\sqrt{x}},\ 0 \le p < \infty; \tag{15}$$

4) compression in the axial and tension in the lateral directions for $P \le 0$, $Q \ge 0$ $(-\infty < \eta \le 0)$

$$f_N(-p,\eta) = \frac{N\left(1-\mathrm{T}_4(-p,\eta)\right)^{N-1}}{2p^2\sqrt{1-\eta}} \lim_{b(p)\to\infty} \int\limits_{p^{-2}\eta^{-2}}^{b(p)} \frac{e^{-x}}{\sqrt{\left(p\sqrt{x}\right)^{-1}-\eta}} \frac{dx}{\sqrt{x}},\ 0 \le -p < \infty. \tag{16}$$

For the partial cases considered above, we obtain the following formulas for the function $f_N(p,\eta)$:

1) the same all-round tension

$$f_N(p,1) = 2N\left(1-F_1(p,1)\right)^{N-1} e^{-p^{-2}} p^{-3},\ 0 \le p < \infty; \tag{17}$$

2) biaxial tension

$$f_N(q,\infty) = \frac{N\left(1-F_1(q,\infty)\right)^{N-1}}{2q^2} \int\limits_{q^{-2}}^{\infty} \frac{e^{-x}}{\sqrt{1-\left(q\sqrt{x}\right)^{-1}}} \frac{dx}{\sqrt{x}},\ 0 \le q < \infty; \tag{18}$$

3) uniaxial tension

$$f_N(p,0)=\frac{N\left(1-F_1(p,0)\right)^{N-1}}{2p^{3/2}}\lim_{b(p)\to\infty}\int_{p^{-2}}^{b(p)}\frac{e^{-x}}{\sqrt[4]{x}}dx,\ 0\le p<\infty; \tag{19}$$

4) tension in the axial and equal compression in the lateral directions

$$f_N(p,-1)=\frac{N\left(1-F_1(p,-1)\right)^{N-1}}{2\sqrt{2}p^2}\lim_{b(p)\to\infty}\int_{p^{-2}}^{b(p)}\frac{e^{-x}}{\sqrt{1+\left(p\sqrt{x}\right)^{-1}}}\frac{dx}{\sqrt{x}},\ 0\le p<\infty; \tag{20}$$

5) compression in the axial and equal tension in the lateral directions

$$f_N(-p,-1)=N\left(1-F_1(-p,-1)\right)^{N-1}\times$$
$$\times\left(\frac{2e^{-p^{-2}}}{p^3}-\frac{1}{2\sqrt{2}p^2}\lim_{b(p)\to\infty}\int_{p^{-2}}^{b(p)}\frac{e^{-x}}{\sqrt{1+\left(p\sqrt{x}\right)^{-1}}}\frac{dx}{\sqrt{x}}\right),\ 0\le -p<\infty. \tag{21}$$

For some partial types of the body stress state with stochastic N crack distribution in Figures 4 and 5, according to relations (17)-(19), graphs of the failure loading probability density distribution $f_N(p,\eta)$ are constructed.

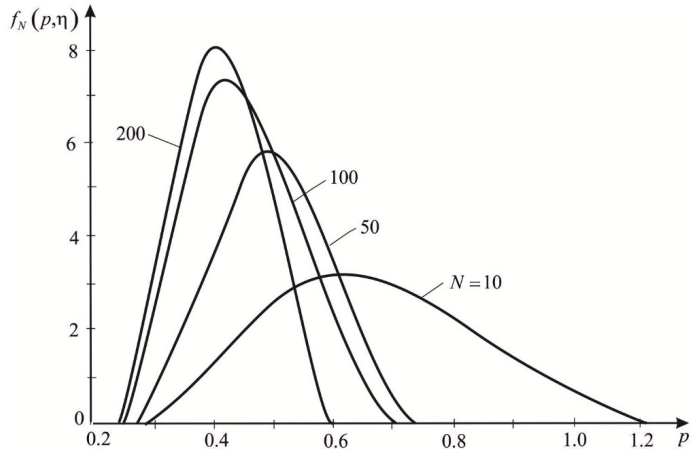

Fig. 4. Failure loading probability density distribution at the same all-round tension for materials with various number of defects

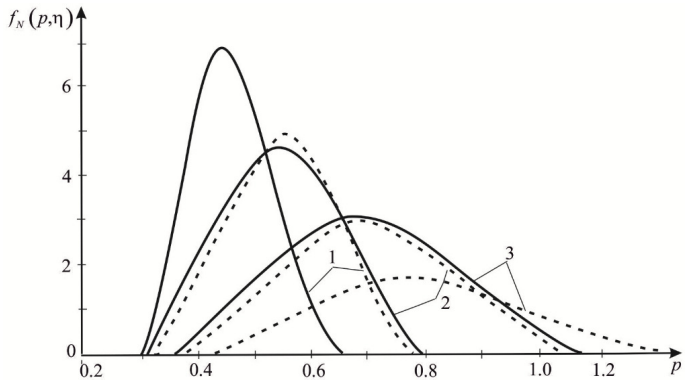

Fig. 5. Failure loading probability density distribution: 1 – the same all-round tension, 2 – biaxial tension, 3 – uniaxial tension; solid for $N = 80$, dashed for $N = 20$

The considered distribution $f_N(p,\eta)$ of a random variable p are unimodal. The minimum value of the failure loading (strength threshold) is zero and does not depend on the type of stress. This means that at an arbitrary (even arbitrarily small) loading there is a non-zero probability of failure.

5. Probabilistic characteristics of failure loading

Consider the probabilistic characteristics of the failure loading (reliability) for a body with a stochastic distribution of N defects and analyze their properties. The most probable value (mode) $Mo(p)$ corresponding to the level loading at which the probability density distribution $f_N(p,\eta)$ reaches a maximum can be found from equation [8]

$$\left(1-F_1(p,\eta)\right)F_1''(p,\eta)+(1-N)(F_1'(p,\eta))^2=0. \tag{22}$$

The failure loading mean value is found from the equation [13]

$$\left\langle p\right\rangle = p_{\min}(\eta)+\int_{p_{\min}(\eta)}^{p_{\max}(\eta)}\left(1-F_1(p,\eta)\right)^N dp. \tag{23}$$

To determine the dispersion of failure loading, apply the formula [13]

$$D(p)=p_{\min}^2(\eta)+2\int_{p_{\min}(\eta)}^{p_{\max}(\eta)}\left(1-F_1(p,\eta)\right)^N p\,dp-\left\langle p\right\rangle^2. \tag{24}$$

Substituting in formulas (22)-(24) expressions for the function $F_1(p,\eta)$ (3)-(6), we obtain the relations for defining the specified probabilistic strength characteristics. In particular, for partial cases (5)-(9) we will have:

1) the same all-round tension

$$\langle p\rangle = \int_0^{\infty}\left(1-e^{-p^{-2}}\right)^N dp; \tag{25}$$

$$D(p) = 2\int_0^{\infty}\left(1-e^{-p^{-2}}\right)^N p\,dp - \left(\int_0^{\infty}\left(1-e^{-p^{-2}}\right)^N dp\right)^2; \tag{26}$$

2) biaxial tension

$$\langle q\rangle = \int_0^{\infty}\left(1-\int_{q^{-2}}^{\infty} e^{-x}\sqrt{1-\left(q\sqrt{x}\right)^{-1}}\,dx\right)^N dq; \tag{27}$$

$$\begin{aligned} D(q) = {} & 2\int_0^{\infty}\left(1-\int_{q^{-2}}^{\infty} e^{-x}\sqrt{1-\left(q\sqrt{x}\right)^{-1}}\,dx\right)^N q\,dq - \\ & -\left(\int_0^{\infty}\left(1-\int_{q^{-2}}^{\infty} e^{-x}\sqrt{1-\left(q\sqrt{x}\right)^{-1}}\,dx\right)^N dq\right)^2; \end{aligned} \tag{28}$$

3) uniaxial tension

$$\langle p\rangle = \int_0^{\infty}\left(1-e^{-p^{-2}}+\int_{p^{-2}}^{\infty} e^{-x}\left(p\sqrt{x}\right)^{-1/2}dx\right)^N dp; \tag{29}$$

$$\begin{aligned} D(p) = {} & 2\int_0^{\infty}\left(1-e^{-p^{-2}}+\int_{p^{-2}}^{\infty} e^{-x}\left(p\sqrt{x}\right)^{-1/2}dx\right)^N p\,dp - \\ & -\left(\int_0^{\infty}\left(1-e^{-p^{-2}}+\int_{p^{-2}}^{\infty} e^{-x}\left(p\sqrt{x}\right)^{-1/2}dx\right)^N dp\right)^2; \end{aligned} \tag{30}$$

4) tension in the axial and equal compression in the lateral directions

$$\langle p\rangle = \int_0^{\infty}\left(1-e^{-p^{-2}}+\frac{1}{\sqrt{2}}\int_{p^{-2}}^{\infty} e^{-x}\sqrt{1+\left(p\sqrt{x}\right)^{-1}}\,dx\right)^N dp; \tag{31}$$

$$\begin{aligned} D(p) = {} & 2\int_0^{\infty}\left(1-e^{-p^{-2}}+\frac{1}{\sqrt{2}}\int_{p^{-2}}^{\infty} e^{-x}\sqrt{1+\left(p\sqrt{x}\right)^{-1}}\,dx\right)^N p\,dp - \\ & -\left(\int_0^{\infty}\left(1-e^{-p^{-2}}+\frac{1}{\sqrt{2}}\int_{p^{-2}}^{\infty} e^{-x}\sqrt{1+\left(p\sqrt{x}\right)^{-1}}\,dx\right)^N dp\right)^2; \end{aligned} \tag{32}$$

5) compression in the axial and equal tension in the lateral directions

$$\langle -p \rangle = \int_0^{\infty} \left(1 - \frac{1}{\sqrt{2}} \int_{p^{-2}}^{\infty} e^{-x} \sqrt{1 + \left(p\sqrt{x} \right)^{-1}} dx \right)^N dp; \tag{33}$$

$$D(-p) = 2\int_0^{\infty} \left(1 - \frac{1}{\sqrt{2}} \int_{p^{-2}}^{\infty} e^{-x} \sqrt{1 + \left(p\sqrt{x} \right)^{-1}} dx \right)^N p\, dp - \\ - \left(\int_0^{\infty} \left(1 - \frac{1}{\sqrt{2}} \int_{p^{-2}}^{\infty} e^{-x} \sqrt{1 + \left(p\sqrt{x} \right)^{-1}} dx \right)^N dp \right)^2. \tag{34}$$

In Figures 6 and 7, in accordance with expressions (25)-(30), graphs of the mean value and dispersion of failure loading for materials with different number of defects N under different types of stress state are considered.

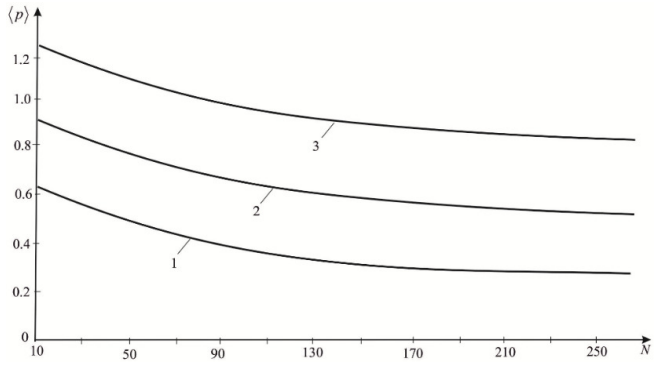

Fig. 6. Failure loading mean value for materials with different number of defects N under different types of stress state: 1 – the same all-round tension, 2 – biaxial tension, 3 – uniaxial tension

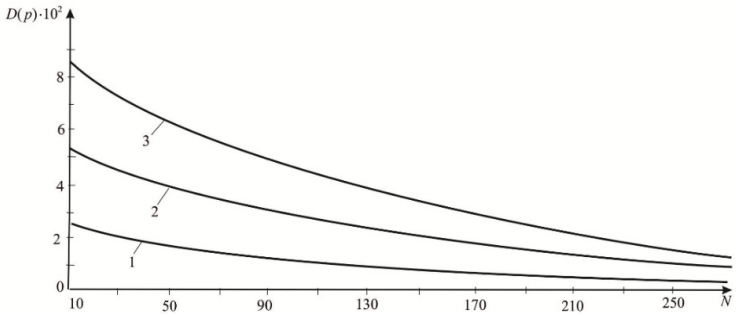

Fig. 7. Failure loading dispersion for materials with different number of defects N under different types of stress state: 1 – the same all-round tension, 2 – biaxial tension, 3 – uniaxial tension

6. Conclusions

With the same all-round tension for the increasing defects number, there is a decrease in the value $Mo(p)$ (Fig. 4). As the parameter N changes, the shape of the failure loading probability density distribution curve $f_N(p,\eta)$ changes. In Figure 5, we observe the applied loading type effect on the body strength. The lowest value $Mo(p)$ will be for the same all-round tension, and the largest for uniaxial tension. Similar regularities are traced in [8]. The change in the $Mo(p)$ magnitude and shape of the failure loading probability density distribution curve depends on the type of stress state and parameter N. The maximum ordinate of the distribution curve depends on the type of applied loading and is directly proportional to the parameter N.

The dependence of the failure loading mean value $\langle p \rangle$ on the type of stress state and the number of defects is shown in Figure 6. For a fixed number of defects, the value $\langle p \rangle$ changes, and its lowest level will be in the case of the same all-round tension. Such patterns are observed in [8]. The number of defects N has almost no effect on the body strength in a certain range of its sizes. As the number of defects increases, the value $\langle p \rangle$ (strength of the body) decreases and asymptotically approaches zero. This phenomenon is known as size effect and is studied in [3, 14].

Dependence of the failure loading dispersion $D(p)$ on the number of cracks and the type of stress state is shown in the Figure 7. The dispersion $D(p)$ is a decreasing function of the parameter N. At a certain interval of change N, we observe a significant decrease in the value $D(p)$, which does not depend on the type of loading. Similar to the case of the mean value $\langle p \rangle$ study, for a certain range of body sizes, the failure loading dispersion $D(p)$ is almost independent of the number of defects.

The identified patterns are consistent with the results of article [15], in which the study of the stochastically defective body strength was based on the failure loading probability distribution function of the Weibull type.

References

[1] Keles, Ö., Garcia, R., & Bowman, K. (2013). Stochastic failure of isotropic, brittle materials with uniform porosity. *Acta Materialia*, *61*(8), 2853-2862. doi: 10.1016/j.actamat.2013.01.024.

[2] Heckmann, K., & Saifi, Q. (2016). Comparative analysis of deterministic and probabilistic fracture mechanical assessment tools. *Kerntechnik*, *81*(5), 484-497. doi: 10.3139/124.110725.

[3] Luo, W., & Bazant, Z. (2017). Fishnet statistics for probabilistic strength and scaling of nacreous imbricated lamellar materials. *Journal of the Mechanics and Physics of Solids*, *109*, 264-287. doi: 10.1016/j.jmps.2017.07.023.

[4] Zhang, T., Yue, R., Wang, X., & Hao, Z. (2018). Failure probability analysis and design comparison of multi-layered sic-based fuel cladding in PWRs. *Nuclear Engineering and Design*, *330*, 463-479. doi: 10.1016/j.nucengdes.2018.02.01.

[5] Zhu, S.P., Hao, Y.Z., & Liao, D. (2020). Probabilistic modeling and simulation of multiple surface crack propagation and coalescence. *Applied Mathematical Modelling*, *78*, 383-398. doi: 10.1016/j.apm.2019.09.045.

[6] He, J., Cui, Y., Liu, Y., & Wang, H. (2020). Probabilistic analysis of crack growth in railway axles using a Gaussian process. *Advances in Mechanical Engineering*, *12*(9), 168781402093603. doi: 10.1177/1687814020936031.

[7] Nejad, R.M., Liu, Z., Ma, W., & Berto, F. (2021). Fatigue reliability assessment of a pearlitic Grade 900A rail steel subjected to multiple cracks. *Engineering Failure Analysis*, *128*, 105625. doi: 10.1016/j.engfailanal.2021.105625.

[8] Kvit, R. (2018). Strength statistical characteristics of the isotropic materials with disc-shaped defects. *Journal of Applied Mathematics and Computational Mechanics*, *17*(4), 25-34. doi: 10.17512/jamcm.2018.4.04.

[9] Fisher, J., & Hollomon, J. (1947). A statistical theory of fracture. *Metals Technology*, *14*(5), 1-16.

[10] Gupta, R.D. & Kundu, D. (2006). On the comparison of Fisher information of the Weibull and GE distributions. *Journal of Statistical Planning and Inference*, *136*(9), 3130-3144. doi: 10.1016/j.jspi.2004.11.013.

[11] Bakoban, R., & Abu-Zinadah, H. (2017). The beta generalized inverted exponential distribution with real data applications. *Statistical Journal*, *15*(1), 65-88. doi: 10.57805/revstat.v15i1.204.

[12] Vytvytsky, P., & Kvit, R. (1990). Probabilistic strength criteria for bodies with stochastically distributed disc-shaped cracks under an axisymmetric stress state. *Physicochemical Mechanics of Materials*, *3*, 53-58 (in Ukrainian).

[13] Vytvytsky, P., & Popina, S. (1980). *Strength and Criteria of Brittle Fracture of Stochastically Defective Bodies.* Kyiv, 186 (in Russian).

[14] Luo, W., & Bazant, Z. (2019). Fishnet statistical size effect on strength of materials with nacreous microstructure. *Journal of Applied Mechanics*, *86*(8), 081006. doi: 10.1115/1.4043663.

[15] Kvit, R. (2018). On the strength of isotropic materials with spatial stochastic distribution of defects. *Precarpathian Bulletin of the Shevchenko Scientific Society*, *1*(45), 100-108 (in Ukrainian).